Integration of clinical data with genome-scale metabolic model of the human adipocyte

Running title: Human adipocyte metabolism at the genome-scale

Adil Mardinoglu[1], Rasmus Agren[1], Caroline Kampf[2], Anna Asplund[2], Intawat Nookaew[1], Peter Jacobson[3], Andrew J. Walley[4], Philippe Froguel[4,5], Lena M. Carlsson[3], Mathias Uhlen[6] and Jens Nielsen[1,*]

[1] Department of Chemical and Biological Engineering, Chalmers University of Technology, Gothenburg, Sweden

[2] Department of Immunology, Genetics and Pathology, Science for Life Laboratory, Uppsala University, Uppsala, Sweden

[3] Department of Molecular and Clinical Medicine and Center for Cardiovascular and Metabolic Research, Sahlgrenska Academy, University of Gothenburg, Gothenburg, Sweden

[4] Department of Genomics of Common Diseases, School of Public Health, Imperial College London, Hammersmith Hospital, London, UK

[5] CNRS 8090-Institute of Biology, Pasteur Institute, Lille, France

[6] Department of Proteomics, School of Biotechnology, AlbaNova University Center, Royal Institute of Technology (KTH), Stockholm, Sweden

* Corresponding author

E-mail: nielsenj@chalmers.se

Tel: +46 31 772 3804

Fax: +46 31 772 3801

Table of Contents

Supplementary Text 3

Adipocyte genome-scale metabolic model coverage on functions 3

Analysis of transcriptome data for subcutaneous adipose tissue and integrated analysis 5

Integration of clinical data into the genome-scale metabolic model for adipocytes 6

Supplementary Tables 7

Table S1. 7

Table S2. 8

Table S3. 8

Table S4. 9

Table S5. 11

Table S6. 11

Table S7. 12

Supplementary Figures 19

Figure S1. 19

Figure S2. 20

Figure S3. 21

Figure S4. 22

Figure S5. 23

Figure S6. 24

Figure S7. 25

Figure S8. 26

Supplementary Datasets 27

Supplementary References 29

Supplementary Text

Adipocyte genome-scale metabolic model coverage on functions

The comprehensive *iAdipocytes1809* covers major known metabolism related pathways as well as extensive knowledge of lipid metabolism in human adipocytes.

Fat absorption and transport to adipocytes: The process of fat digestion is complex and involves multi coordination of lingual, gastric, intestinal, biliary and pancreatic functions. The short and medium-chain FAs resulting from the digestion process are absorbed in the gut and then transported to the liver, via the portal vein, where it is oxidized. Other yields of the digestion process including long-chain FAs, monoacylglycerol (MAG), lysophospholipids and cholesterols are combined with bile salts and absorbed by the intestine wall. The long-chain FAs are converted to TAGs as well as cholesterol and lysophospholipids are converted to their esters in the intestine and recently formed TAGs, phospholipids (PLs) and esters are combined into *de novo* synthesized apolipoproteins to form chylomicrons. Produced chylomicrons in enterocytes are transported to the bloodstream via the lymph vessels and they are to be used as FA source by the adipose and other soft tissues.

Chylomicrons in the bloodstream are hydrolyzed to MAG, FAs, and glycerol by lipoprotein lipase (LPL) to be stored as TAGs in adipocytes or to be used as an energy source. Although small amount of FAs are synthesized by *de novo* FA synthesis inside the cell, most of the FAs deposited in adipocytes are taken up from two potential sources: non-esterified FAs (NEFAs) and lipoproteins (Table S5) including chylomicrons, very-low-density lipoprotein (VLDL), low-density lipoproteins (LDL) and high-density lipoproteins (HDL) through LPL (Duncan et al., 2007; Guilherme et al., 2008; Large et al., 2004). There is a clear preference for uptake of FAs from lipoproteins compared to plasma NEFAs whereas chylomicrons are a better source of FAs in the post-prandial state and VLDLs are a better source of FAs in post-absorptive state (Bickerton et al., 2007; Large et al., 2004). After the removal of the FAs in chylomicrons by adipocytes, remnants of chylomicrons are cleared from the blood by the liver LDL receptors and their related proteins. The liver catabolizes chylomicrons remnants, forms VLDL by combining resynthesized TAGs with small amounts of cholesterol and PLs and releases them into the blood to be used as FAs sources for adipocytes in the post-absorptive state. FAs in VLDL are taken up through LPL hydrolysis by adipocytes and remnants of VLDL are cleared by the liver to be transformed into intermediate-density lipoproteins (IDL) and finally into LDL.

Adipose tissue stores more than 25% of the total body cholesterol and *de novo* synthesized cholesterol and cholesterol taken up via lipoproteins are integrated into the plasma membrane and lipid droplets (LD) structure. In adipocytes, *de novo* cholesterol synthesis is limited and the greater part of the cholesterol in the cell is taken up from lipoproteins through LPL hydrolysis. LDL and HDL are the potential carriers for cholesterol and CEs from plasma to adipocytes where CEs are hydrolyzed to free cholesterols and re-esterified.

In the reconstructed GEM for adipocytes, 59 different common long and very long chain FAs (Table S4) in human plasma can be taken up as NEFAs and lipoproteins (Figure S5, S6 and

S7). Cholesterol and its 59 different CEs can also be taken up from LDLs and HDLs. In the post-prandial state, FAs and CEs can be incorporated into LD structures and in the post-absorptive state LDs can be broken down to FAs and CEs.

De novo synthesis of fatty acids: Even though factors such as background diet, physical activity, genetics and hormones can influence *de novo* FAs synthesis, synthetic processes are quite limited in adipocytes. The main sources of the glycerol-3-phosphate for FA synthesis are glucose that is taken up from blood by the insulin-regulated GLUT-4 transporter, lactate/pyruvate that can be converted to glycerol-3-phosphate via glyceroneogenesis, and from catabolism of amino acids. The synthetic process starts with the breakdown of the excess dietary carbohydrates to acetyl-CoA that is a precursor for biosynthesis of palmitic acid (C:16:0). Palmitic acid can be further elongated to longer chain saturated FAs by adding acetyl groups, through the action of FA elongation systems in the cytoplasm. In mammalian systems, desaturation of *de novo* synthesized saturated FAs stops with the formation of the n-9 series monounsaturated fatty acids (MUFA) performed by Δ9 desaturase. The products of *de novo* synthesis are esterified with glycerol to form TAGs and the TAGs are stored in LDs. A healthy subject has the capacity of synthesizing about 20% percent of the FAs in newly formed TAGs via *de novo* synthesis and this knowledge is used in the formation of LDs in the model (Strawford et al., 2004).

In the GEM, with the uptake of the essential FAs linoleate and linolenate, 57 different long and very long chain FAs can be synthesized and can be incorporated into the formation of LDs.

Metabolism of linoleate and linolenate: linoleate (LA), unsaturated omega-6 fatty acid, and linolenate (ALA), polyunsaturated omega-3 fatty acid cannot be synthesized by mammalian systems since mammals cannot introduce double bonds between Δ10 and the methyl terminal end. LA and ALA are essential FAs for the synthesis of arachidonate (AA) and eicosapentaenoate (EPA), that serve as precursors for long-chain polyunsaturated fatty acids (LCPUFAs) and eicosanoids and they must be obtained from the diet. After the uptake of LA and ALA, different steps are involved as follows: double bond is inserted at the Δ6 position of LA and ALA by the action of Δ6 desaturase, two carbon chains are elongated, another double bond is inserted at the Δ5 position by Δ5-desaturase to form AA (20:4n-6) and EPA (20:5n-3), two carbon chain is elongated to form 22:4n-6 and 22:5n-3, and further two carbon chains are elongated to produce 24:4n-6 and 24:5n-3, respectively. Subsequently, 24:4n-6 and 24:5n-3 are desaturated by Δ6 desaturase to yield 24:5n-6 and 24:6n-3 that are shortened two carbon chain by the beta oxidation in the peroxisome to form docosapentaenoic acid (DPA) and docosahexaenoic acid (DHA). The LA and ALA pathways are independent of each other and there are no crossover reactions between them. There is, however, a competition between the two pathways as the reactions in both pathways are catalyzed by the same enzymes (Figure S6).

In the GEM, the eicosanoids such as prostaglandins (PG), prostacyclins (PGI), thromboxanes (TX), leukotrienes (LT), hydroperoxytetraenoic acids (HPETE), hydroxyeicosatetraenoic acids (HETE) and lipoxins are formed via long-chain omega-6 and omega-3 C20 PUFA. This

biological function is performed by two different enzymes such as Cyclooxygenase (COX) enzyme that converts the C20 FAs to prostanoids including PG, PGI and TX and lipooxygenase (LOX) enzyme that converts the C20 FAs to HPETE and further to LT, HETE and lipoxins. There are also two isoforms of COX enzymes including COX 1 that controls the physiological roles of eicosanoids, and COX 2 which is activated by some biological processes such as inflammation. DHA-derived signaling molecules docosanoids have also been formed via LA and ALA pathways by COX-2 and 5-LOX enzymes. Docosanoids are also termed as D-series resolvins and protectins (neuroprotectins D1) that are both neuroprotective and anti-inflammatory. In addition, both the eicosanoids and the docosanoids are involved in different biological processes such as inflammation, immune response and cell growth and proliferation. Omega-3 and Omega-6 FAs regulates the enzymes that perform the lipid metabolism (i.e. inhibit FA synthesis in adipose tissue and contain transcription of the leptin gene that regulates appetite, body weight and adiposity) whereas omega-3 FAs have a number of other anti-inflammatory effects via cytokines family of proteins.

Oxidation of fatty acids: During starvation, the TAGs in which the body stores energy provide FAs as a direct energy source for other tissues and a substrate for production of ketone bodies. In the model, β-oxidation of LCFA occurs in the mitochondria and β-oxidation of VLCFA starts in the peroxisome and continues either in the peroxisome or the mitochondria. Transport of FAs (acyl-CoA) into the mitochondria requires the four step carnitine shuttle whereas transport to the peroxisome does not. In the model, phytanic acid that is taken up from the blood cannot undergo β-oxidation due to its β-methyl branch. Therefore, it is broken down into pristanic acid by removal of a single carbon from the carboxyl end via α-oxidation that takes place in the peroxisome.

Other Major Metabolic Pathways: Adipose tissue takes up glucose in the post-prandial and post-absorptive state (McQuaid et al., 2011) and most of the glucose taken up by adipocytes enters glycolysis, which is an important pathway for TAGs synthesis by providing glycerol-3-phosphate necessary for FAs esterification. Some part of the glucose may also enter the tricarboxylic acid cycle (TCA cycle) for energy production.

Analysis of transcriptome data for subcutaneous adipose tissue and integrated analysis
Gene expression in subcutaneous adipose tissue (SAT) of subjects involved in Swedish Obese Subjects (SOS) Sip Pair Study (Table S1) was analyzed. Gene expression levels of overweight and obese groups are compared with the lean group and the Limma package was used to identify significant genes that were over- or under expressed (adjusted p-values cutoff level < 0.001). Linear models were fitted to the data using linear and robust regression separately before applying an empirical Bayes shrinkage method. Correction for multiple testing was performed using Storey's FDR procedure on the p-values of the shrunk test statistics to generate q-values. The q-values, generated for each probe set in each group were calculated using the Reporter algorithm (Oliveira et al., 2008; Patil and Nielsen, 2005) in order to summarize the transcriptional changes in terms of more general features such as biological process Gene Ontology (BP:GO) terms (Berardini et al., 2010) and KEGG pathways (Kanehisa et al., 2012). Figures S1 and S2 show the output for KEGG pathways for male and female subjects, respectively (cutoff p <1e-04). Figures S3 and S4 show the output for BP:GO

for male and female subjects, respectively (cutoff p <1e-04). During the mapping of the probe-sets to the KEGG pathways and BP:GO terms, the manufacturer mapping file was used.

Integration of clinical data into the genome-scale metabolic model for adipocytes

In order to reconstruct a predictive and functional model for adipocytes in white adipose tissue (WAT), it is necessary to incorporate some relevant experimental measurements (i.e. Fatty Acid (FA) composition of plasma and WAT). Mitrou et. al. (Mitrou et al., 2009) investigated insulin action on glucose disposal in SAT and muscle tissue after the consumption of a mixed meal in different healthy subject groups. The study consisted of 30 obese non-diabetic women (age 34±1 year, body mass index (BMI) 47±1 kg/m²) and 10 lean women (age 39±4 year, BMI 23±1 kg/m²). The glucose and insulin levels were measured at the veins draining the abdominal SAT and forearm muscles and in the radial artery for 360 min. Fasting TAGs was increased in obese subjects (1.56±0.2 mmol/l) versus lean subjects (0.93±0.1 mmol/l) and HDL-cholesterol was decreased in obese subjects (0.95±0.05 mmol/l) versus lean subjects (1.2±0.07mmol/l). Total cholesterol and LDL-cholesterol are also increased in obese subjects (5.3±0.4 mmol/l and 3.7±0.4 mmol/l) versus lean subjects (4.4±0.2 mmol/l and 2.8±0.2 mmol/l). In post-prandial state, glucose uptake in SAT in obese subjects is less than lean subjects (0.45±0.1 versus 1.1±0.17 µmol/min per 100 ml tissue). However, the average glucose uptake rate in obese subjects (0.275±0.04 mmol/min) is more than lean subjects (0.12±0.02 mmol/min) when SAT glucose uptake was multiplied by tissue mass and expressed as per total fat mass. In obese subjects, plasma insulin level is increased comparing to lean subjects and the glucose uptake rate in SAT is not altered in both post-prandial and post-absorptive states (approximately 0.45 µmol/min per 100 ml tissues).

Bickerton et. al. (Bickerton et al., 2007) probe the components of fat metabolism in post-prandial and post-absorptive states by using a combination of stable isotope labeling and arteriovenous difference measurements. The uptake of the FAs derived from chylomicron-TAGs, VLDL-TAGs and circulating NEFAs are quantified in adipose tissue and skeletal muscle. In post-prandial state, the adipose tissue takes up FAs from both dietary (chylomicron) and VLDL-TAGs with greater fractional extraction of the chylomicron-TAGs. Significant amount of plasma NEFAs that are minor in comparison to chylomicron-TAGs FAs are also taken up in the post-prandial state but not in the post-absorptive state. In the late post-absorptive state (6 hours after meal), adipose tissue NEFA uptake rate of the LPL-derived fatty acids (~320 nmol/min per 100 g tissues) and plasma NEFA (~-180 nmol/min per 100 g tissues) is reported and used in our study.

Supplementary Tables

Table S1. Clinical data for lean and obese subjects obtained from Swedish Obese Subjects (SOS) Sib Pair Study (Walley et al., 2012). In the SOS Sib Pair Study, human subcutaneous adipose tissue (SAT) samples are obtained from subjects in order to understand the molecular mechanism of the obesity since SAT displays obesity-related changes in gene expression (Wellen and Hotamisligil, 2003). In the SOS Sib Pair Study, in post-absorptive state, the measurements of anthropometry, fat mass (FM), fat-free mass (FFM), blood pressure (BP), fasting glucose, total cholesterol, triacylglycerols, high-density lipoprotein cholesterol (HDL-cholesterol), low-density lipoprotein cholesterol (LDL-cholesterol), serum insulin, serum C peptide (C-peptide), and highly sensitive Creactive protein (hs-CRP) were performed. Values are given as means ± SD unless stated otherwise.

Obesity-discordant Sib-pair study, a sub-study of the Swedish Obese Subjects study						
	FEMALE			**MALE**		
Variable/Group	**Lean**	**Overweight**	***Obese***	**Lean**	**Overweight**	**Obese**
BMI Range (kg/m2)	18.5< BMI< 25	25≤ BMI<30	*30 ≤ BMI*	18.5< BMI< 25	25≤ BMI<30	30 ≤ BMI
Sample size (n)	112	17	80	42	33	20
Age	36.5 ± 7.6	38.5 ± 6.6	37.5 ± 6.7	34.3 ± 8.9	37.9 ± 6.9	36.9 ± 9.4
BMI (kg/m2)	22.0 ± 1.5	27.2 ± 1.6	37.0 ± 4.3	22.2 ± 1.6	27.4 ± 1.3	35.8 ± 5.1
Waist	76.0 ± 5.4	91.2 ± 6.8	110.4 ± 10	81.6 ± 5.6	94.8 ± 4.8	117.1 ± 11.1
WHR	0.79 ± 0.05	0.86 ± 0.06	0.92 ± 0.07	0.85 ± 0.05	0.91 ± 0.05	0.99 ± 0.06
FFM (kg)	48.6 ± 4.8	52.7 ± 5.1	59.4 ± 5.7	64.1 ± 7.0	71.6 ± 7.3	77.9 ± 7.2
FM (kg)	14.9 ± 4.3	24.4 ± 5.1	41.9 ± 8.2	10.9 ± 5.0	19.2 ± 6.2	36.1 ± 8.2
Systolic BP (mmHg)	105.8 ± 9.7	109.3 ± 10.2	115.9 ± 11.3	114.6 ± 9.3	118.0 ± 9.6	117.3 ± 14.6
Diastolic BP (mmHg)	64.7 ± 8.7	67.2 ± 8.8	71.2 ± 7.9	69.0 ± 8.3	68.7 ± 9.0	72.4 ± 9.5
Insulin (mU/l)	5.07 ± 1.91	7.51 ± 2.64	11.58 ± 6.41	6.03 ± 3.46	7.33 ± 2.69	14.01 ± 8.98
HOMA-IR	1.04 ± 0.41	1.55 ± 0.58	2.48 ± 1.45	1.31 ± 0.78	1.66 ± 0.66	3.17 ± 2.03
C-peptide (mmol/l)	0.46 ± 0.14	0.60 ± 0.11	0.83 ± 0.26	0.52 ± 0.17	0.64 ± 0.25	0.98 ± 0.44
Hs-CRP (mg/l)	1.90 ± 4.87	2.69 ± 2.42	7.55 ± 8.30	1.46 ± 2.77	1.76 ± 2.32	4.44 ± 3.40
Glucose (mmol/l)	4.60 ± 0.36	4.63 ± 0.37	4.78 ± 0.44	4.83 ± 0.41	5.06 ± 0.51	5.11 ± 0.55
Triacylglycerol (mmol/l)	0.69 ± 0.30	0.91 ± 0.30	1.00 ± 0.32	0.82 ± 0.39	1.53 ± 1.25	1.18 ± 0.52
Total Cholesterol (mmol/l)	4.13 ± 0.86	4.23 ± 0.91	4.43 ± 0.67	4.03 ± 1.01	5.00 ± 1.02	4.48 ± 0.69
LDL-cholesterol (mmol/l)	2.37 ± 0.65	2.61 ± 0.82	2.77 ± 0.60	2.50 ± 0.68	3.24 ± 0.97	2.82 ± 0.50
HDL-cholesterol (mmol/l)	1.45 ± 0.36	1.28 ± 0.30	1.21 ± 0.28	1.21 ± 0.35	1.14 ± 0.22	1.11 ± 0.21

Table S2. Versions of the databases used in the reconstruction of the Human Metabolic Reaction (HMR) database and genome-scale metabolic model for adipocytes, *iAdipocytes1809*.

Database	Export format	Version	Downloaded from
Recon 1	Flat file, SBML	Jan 31, 2008	http://bigg.ucsd.edu/
EHMN	Flat file	June 6, 2009	http://www.ehmn.bioinformatics.ed.ac.uk/
HepatoNet1	Flat file	March 1, 2011	http://www.nature.com/msb/journal/
Reactome	Flat file, SBML	October 17, 2011	http://www.reactome.org/
HumanCyc	Flat file, SBML	15.5	http://biocyc.org/download.shtml/
KEGG	Flat file, KGML	48	ftp://ftp.genome.jp/pub/kegg/
HPA	Flat file	10	http://www.proteinatlas.org/
Uniprot	Flat file	January 9, 2012	http://www.uniprot.org/
HMDB	Flat file	2.4	http://www.hmdb.ca/
LipidMap	Flat file	November 9, 2011	http://www.lipidmaps.org/

Table S3. Content of genome-scale metabolic model for adipocytes, *iAdipocytes1809*, Human Metabolic Reaction (HMR) database and previously published literature-based models.

GEMs	Reactions	Metabolites	Genes
iAdipocytes1809	6160	4550 (2497)*	1809
Human Metabolic Reaction (HMR) database	8100	6000 (3160)*	3668
iHuman1512	5535	3397	1512
Recon 1	3402	2785	1477
EHMN	6216	2678	2482
HepatoNet1	2519	777	713
iAB586	649	493	586

* unique metabolites in the model.

Table S4. List of the fatty acids used in the genome-scale metabolic model for adipocytes, *iAdipocytes1809*.

ID	LM_ID	SYSTEMATIC_NAME	OUR_MODEL_NAME	SYNONYMS
1	LMFA01010012	Dodecanoic acid	lauric acid	Lauric acid (C12:0)
2	LMFA01010013	Tridecanoic acid	tridecylic acid	Tridecylic acid(C13:0)
3	LMFA01010014	Tetradecanoic acid	myristic acid	Myristic acid (C14:0)
4	LMFA01030250	9E-tetradecenoic acid	(9E)-tetradecenoic acid	Myristoleic acid (C14:1,n-5)
5	LMFA01030249	7Z-tetradecenoic acid	(7Z)-tetradecenoic acid	Tetradecenoic acid (C14:1,n-7)
6	LMFA01030049	5Z-tetradecenoic acid	physeteric acid	Physeteric acid (C14:1,n-9)
7	LMFA01010015	Pentadecanoic acid	pentadecylic acid	Pentadecanoic acid (C15:0)
8	LMFA01010001	Hexadecanoic acid	palmitate	Palmitic acid (C16:0)
9	LMFA01030056	9Z-hexadecenoic acid	palmitolate	Hexadecenoic acid (C16:1,n-7)
10	LMFA01030055	7Z-hexadecenoic acid	7-palmitoleic acid	Hexadecenoic acid (C16:1,n-9)
11	LMFA01010017	Heptadecanoic acid	margaric acid	Margaric acid (C17:0)
12	LMFA01030283	10Z-heptadecenoic acid	(10Z)-heptadecenoic acid	Heptadecenoic acid (C17:1,n-7)
13	LMFA01030060	9Z-heptadecenoic acid	9-heptadecylenic acid	Heptadecenoic acid (C17:1,n-8)
14	LMFA01010018	Octadecanoic acid	stearate	Stearic acid (C18:0)
15	LMFA01030290	13Z-octadecenoic acid	(13Z)-octadecenoic acid	Octadecenoic acid (C18:1,n-5)
16	LMFA01030076	11Z-octadecenoic acid	cis-vaccenic acid	Octadecenoic acid (C18:1,n-7)
17	LMFA01030002	9Z-octadecenoic acid	oleate	Oleic acid (C18:1,n-9)
18	LMFA01030073	9E-octadecenoic acid	elaidate	Elaidic acid (C18:1,n-9)
19	LMFA01030068	7Z-octadecenoic acid	(7Z)-octadecenoic acid	Octadecenoic acid (C18:1,n-11)
20	LMFA01030332	6Z,9Z-octadecadienoic acid	(6Z,9Z)-octadecadienoic acid	Isolinoleic acid (C18:2,n-9)
21	LMFA01010019	Nonadecanoic acid	nonadecylic acid	Nonadecylic acid(C19:0)
22	LMFA01010020	Eicosanoic acid	eicosanoate	Eicosanoic acid (C20:0)
23	LMFA01030367	13Z-eicosenoic acid	(13Z)-eicosenoic acid	Eicosenoic acid (C20:1,n-7)
24	LMFA01030085	11Z-eicosenoic acid	cis-gondoic acid	Eicosenoic acid (C20:1,n-9)
25	LMFA01030700	9Z-eicosenoic acid	9-eicosenoic acid	Eicosenoic acid (C20:1,n-11)
26	LMFA01030376	8Z,11Z-eicosadienoic acid	8,11-eicosadienoic acid	Eicosadienoic acid (C20:2,n-9)
27	LMFA01030157	5,8,11-eicosatrienoic acid	mead acid	Mead acid (C20:3,n-9)
28	LMFA01010021	Heneicosanoic acid	henicosanoic acid	Henicosanoic acid(C21:0)
29	LMFA01010022	Docosanoic acid	behenic acid	Behenic acid (C22:0)

30	LMFA01030089	13Z-docosenoic acid	cis-erucic acid	Docosenoic acid (C22:1,n-9)
31	LMFA01030088	11Z-docosenoic acid	cis-cetoleic acid	Docosenoic acid (C22:1,n-11)
32	LMFA01010023	Tricosanoic acid	tricosanoic acid	Tricosanoic-acid (C23:0)
33	LMFA01010024	Tetracosanoic acid	lignocerate	Lignoceric acid (C24:0)
34	LMFA01030092	15Z-tetracosenoic acid	nervonic acid	Nervonic acid (C24:1,n-9)
35	LMFA01010026	Hexacosanoic acid	cerotic acid	Cerotic acid (C26:0)
36	LMFA01030095	17Z-hexacosenoic acid	ximenic acid	Ximenic acid (C26:1,n-9)
37	LMFA01030152	9Z,12Z,15Z-octadecatrienoic acid	linolenate	Linolenic acid (C18:3,n-3)*
38	LMFA01030357	6Z,9Z,12Z,15Z-octadecatetraenoic acid	stearidonic acid	Stearidonic-acid (C18:4,n-3)
39	LMFA01030176	8Z,11Z,14Z,17Z-eicosatetraenoic acid	omega-3-arachidonic acid	Eicosatetraenoic acid (C20:4,n-3)
40	LMFA01030759	5Z,8Z,11Z,14Z,17Z-eicosapentaenoic acid	EPA	Timnodonic acid (C20:5,n-3)
41	LMFA04000044	7Z,10Z,13Z,16Z,19Z-docosapentaenoic acid	DPA	Clupanodonic acid (C22:5,n-3)
42	LMFA01030821	9Z,12Z,15Z,18Z,21Z-tetracosapentaenoic acid	(9Z,12Z,15Z,18Z,21Z)-TPA	Tetracosapentaenoic acid (C24:5,n-3)
43	LMFA01030822	6Z,9Z,12Z,15Z,18Z,21Z-tetracosahexaenoic acid	(6Z,9Z,12Z,15Z,18Z,21Z)-THA	Tetracosahexaenoic acid (C24:6,n-3)
44	LMFA01030185	4Z,7Z,10Z,13Z,16Z,19Z-docosahexaenoic acid	DHA	Docosahexaenoic acid (C22:6, n-3)
45	LMFA01030378	11Z,14Z,17Z-eicosatrienoic acid	(11Z,14Z,17Z)-eicosatrienoic acid	Eicosatrienoic acid (C20:3,n-3)
46	LMFA01030407	13Z,16Z,19Z-docosatrienoic acid	13,16,19-docosatrienoic acid	Docosatrienoic-acid(C22:3,n-3)
47	N/A	10Z,13Z,16Z,19Z-docosatetraenoic acid	10,13,16,19-docosatetraenoic acid	Docosatetraenoic acid C(22:4,n-3)
48	N/A	12Z,15Z,18Z,21Z-tetracosatetraenoic acid	12,15,18,21-tetracosatetraenoic acid	Tetracosatetraenoic acid C(24:4,n-3)
49	LMFA01030120	9Z,12Z-octadecadienoic acid	linoleate	Linoleic acid (C18:2, n-6)*
50	LMFA01030141	6Z,9Z,12Z-octadecatrienoic acid	gamma-linolenate	Gamolenic acid (C18:3,n-6)
51	LMFA01030158	8Z,11Z,14Z-eicosatrienoic acid	dihomo-gamma-linolenate	Eicosatrienoic acid (C20:3,n-6)
52	LMFA01030001	5Z,8Z,11Z,14Z-eicosatetraenoic acid	arachidonate	Arachidonic acid (C20:4,n-6)
53	LMFA01030178	7Z,10Z,13Z,16Z-docosatetraenoic acid	adrenic acid	Adrenic acid (C22:4,n-6)
54	LMFA01030819	9Z,12Z,15Z,18Z-tetracosatetraenoic acid	(9Z,12Z,15Z,18Z)-TTA	Tetracosatetraenoic acid (C24:4,n-6)
55	LMFA01030820	6Z,9Z,12Z,15Z,18Z-tetracosapentaenoic acid	(6Z,9Z,12Z,15Z,18Z)-TPA	Tetracosapentaenoic acid (C24:5,n-6)
56	LMFA04000064	4Z,7Z,10Z,13Z,16Z-docosapentaenoic acid	(4Z,7Z,10Z,13Z,16Z)-DPA	Docosapentaenoic acid (C22:5,n-6)
57	LMFA01030130	11Z,14Z-eicosadienoic acid	(11Z,14Z)-eicosadienoic acid	Eicosadienoic acid (C20:2,n-6)
58	LMFA01030405	13Z,16Z-docosadienoic acid	(13Z,16Z)-docosadienoic acid	Docosadienoic acid (C22:2,n-6)
59	LMFA01030685	10Z,13Z,16Z-docosatriynoic acid	10,13,16-docosatriynoic acid	Docosatriynoic acid (C22:3,n-6)

Table S5. Lipid composition of plasma lipoproteins that are fatty acid and cholesterol source for adipocytes (Caballero, 2009; Mills et al., 1984).

Lipoproteins	Composition (wt%)					Size (nm)	Origin
	Cholesterol	CE	TAGs	Phospholipids	Protein		
Chylomicrons	1	3	90	4	2	100-400	Intestine
VLDL	7	14	55	16	8	40-70	Liver
IDL	6	22	30	24	18	30-40	VLDL
LDL	7	48	5	20	20	22.5-27.5	VLDL & IDL
HDL	4	15	4	27	50	7.5-10	Liver & Intestine

Table S6. Lipid composition of lipid droplets (LDs) in adipocytes (Bartz et al., 2007). LDs are rich in triacylglycerols (TAGs), cholesterol esters (CEs) and an unknown neutral lipid (~19%) that migrated between CEs and TAGs, ether neutral lipid monoalk(en)yl diacylglycerol (MADAG). LDs also contain phospholipids including phosphatidylcholine (PC), phosphatidylethanolamine (PE), phosphatidylinositol (PI), ether-linked phosphatidylcholine (ePC), ether-linked phosphatidylethanolamine (ePE), lyso phosphatidylcholine (LPC), lysophosphatidylethanolamine (LPE) and small amount of phosphatidylserine (PS) or sphingomyelin (SM).

		Relative amount of lipid (%)	Phospholipids (%)
TAGs		44.0	
CE		34.0	
MADAG		19.0	
NEFAs		0.5	
Cholesterol		0.5	
Phospholipids		2.0	
	PC	0.92	46
	PE	0.34	17
	PI	0.16	8
	PS	0.02	1
	SM	0.04	2
	ePC	0.24	12
	ePE	0.08	4
	LPC	0.06	3
	LPE	0.14	7

Table S7. Random sampling algorithm results for obese subjects compared to lean subjects. Reactions change both in flux and expression in the same direction. DW: Down regulated.

Reaction	RXNID	Male	Female	EQUATION	SUBSYSTEM
DW: HMR_0005	HMR_0005	0.97519	1	1-acylglycerol-chylomicron pool[c] + H2O[c] => fatty acid-LD-TG1 pool[c] + glycerol[c]	Acylglycerides metabolism
DW: HMR_0002	HMR_0002	0.96473	1	H2O[s] + TAG-chylomicron pool[s] => 1,2-diacylglycerol-chylomicron pool[s] + fatty acid-chylomicron pool[s]	Acylglycerides metabolism
DW: HMR_0003	HMR_0003	0.96473	1	1,2-diacylglycerol-chylomicron pool[s] + H2O[s] => 1-acylglycerol-chylomicron pool[s] + fatty acid-chylomicron pool[s]	Acylglycerides metabolism
DW: HMR_0010	HMR_0010	0.97519	1	1-acylglycerol-VLDL pool[c] + H2O[c] => fatty acid-LD-TG1 pool[c] + glycerol[c]	Artificial reactions
DW: HMR_3275	HMR_3275	0.78951	0.78409	FAD[m] + linoleoyl-CoA[m] => FADH2[m] + trans,cis,cis-2,9,12-octadecatrienoyl-CoA[m]	Beta oxidation of di-unsaturated fatty acids (n-6) (mitochondrial)
DW: HMR_3278	HMR_3278	0.791	0.7841	(3S)-3-hydroxylinoleoyl-CoA[m] + NAD+[m] => 3-oxolinoleoyl-CoA[m] + H+[m] + NADH[m]	Beta oxidation of di-unsaturated fatty acids (n-6) (mitochondrial)
DW: HMR_3279	HMR_3279	0.79028	0.7841	3-oxolinoleoyl-CoA[m] + CoA[m] => acetyl-CoA[m] + cis,cis-palmito-7,10-dienoyl-CoA[m]	Beta oxidation of di-unsaturated fatty acids (n-6) (mitochondrial)
DW: HMR_3280	HMR_3280	0.78951	0.78409	FAD[m] + cis,cis-palmito-7,10-dienoyl-CoA[m] => FADH2[m] + trans,cis,cis-2,7,10-hexadecatrienoyl-CoA[m]	Beta oxidation of di-unsaturated fatty acids (n-6) (mitochondrial)
DW: HMR_3277	HMR_3277	0.78682	0.7841	H2O[m] + trans,cis,cis-2,9,12-octadecatrienoyl-CoA[m] => (3S)-3-hydroxylinoleoyl-CoA[m]	Beta oxidation of di-unsaturated fatty acids (n-6) (mitochondrial)
DW: HMR_3288	HMR_3288	0.72685	0.72411	cis,cis-3,6-dodecadienoyl-CoA[m] => trans,cis-lauro-2,6-dienoyl-CoA[m]	Beta oxidation of di-unsaturated fatty acids (n-6) (mitochondrial)
DW: HMR_3282	HMR_3282	0.72685	0.72411	(3S)-3-hydroxy-cis,cis-palmito-7,10-dienoyl-CoA[m] + NAD+[m] => 3-oxo-cis,cis-7,10-hexadecadienoyl-CoA[m] + H+[m] + NADH[m]	Beta oxidation of di-unsaturated fatty acids (n-6) (mitochondrial)
DW: HMR_3286	HMR_3286	0.72685	0.72411	3(S)-hydroxy-(5Z,8Z)-tetradecadienoyl-CoA[m] + NAD+[m] => 3-oxo-cis,cis-5,8-tetradecadienoyl-CoA[m] + H+[m] + NADH[m]	Beta oxidation of di-unsaturated fatty acids (n-6) (mitochondrial)
DW: HMR_3292	HMR_3292	0.72685	0.72411	(3S)-3-hydroxydodec-cis-6-enoyl-CoA[m] + NAD+[m] => 3-oxolaur-6-cis-enoyl-CoA[m] + H+[m] + NADH[m]	Beta oxidation of di-unsaturated fatty acids (n-6) (mitochondrial)
DW: HMR_3298	HMR_3298	0.72685	0.72411	(2E)-decenoyl-CoA[m] <=> trans-3-decenoyl-CoA[m]	Beta oxidation of di-unsaturated fatty acids (n-6) (mitochondrial)
DW: HMR_3293	HMR_3293	0.72663	0.72411	3-oxolaur-6-cis-enoyl-CoA[m] + CoA[m] => 4-cis-decenoyl-CoA[m] + acetyl-CoA[m]	Beta oxidation of di-unsaturated fatty acids (n-6) (mitochondrial)

DW: HMR_3283	HMR_3283	0.72619	0.72411	3-oxo-cis,cis-7,10-hexadecadienoyl-CoA[m] + CoA[m] => acetyl-CoA[m] + cis,cis-myristo-5,8-dienoyl-CoA[m]	Beta oxidation of di-unsaturated fatty acids (n-6) (mitochondrial)
DW: HMR_3287	HMR_3287	0.72619	0.72411	3-oxo-cis,cis-5,8-tetradecadienoyl-CoA[m] + CoA[m] => acetyl-CoA[m] + cis,cis-3,6-dodecadienoyl-CoA[m]	Beta oxidation of di-unsaturated fatty acids (n-6) (mitochondrial)
DW: HMR_3284	HMR_3284	0.72549	0.7241	FAD[m] + cis,cis-myristo-5,8-dienoyl-CoA[m] => FADH2[m] + trans-2-cis,cis-5,8-tetradecatrienoyl-CoA[m]	Beta oxidation of di-unsaturated fatty acids (n-6) (mitochondrial)
DW: HMR_3296	HMR_3296	0.72453	0.72409	2-trans-4-cis-decadienoyl-CoA[m] + H+[m] + NADH[m] => NAD+[m] + trans-3-decenoyl-CoA[m]	Beta oxidation of di-unsaturated fatty acids (n-6) (mitochondrial)
DW: HMR_3281	HMR_3281	0.72301	0.72411	H2O[m] + trans,cis,cis-2,7,10-hexadecatrienoyl-CoA[m] => (3S)-3-hydroxy-cis,cis-palmito-7,10-dienoyl-CoA[m]	Beta oxidation of di-unsaturated fatty acids (n-6) (mitochondrial)
DW: HMR_3285	HMR_3285	0.72301	0.72411	H2O[m] + trans-2-cis,cis-5,8-tetradecatrienoyl-CoA[m] => 3(S)-hydroxy-(5Z,8Z)-tetradecadienoyl-CoA[m]	Beta oxidation of di-unsaturated fatty acids (n-6) (mitochondrial)
DW: HMR_3290	HMR_3290	0.72301	0.72411	H2O[m] + trans,cis-lauro-2,6-dienoyl-CoA[m] => (3S)-3-hydroxydodec-cis-6-enoyl-CoA[m]	Beta oxidation of di-unsaturated fatty acids (n-6) (mitochondrial)
DW: HMR_3429	HMR_3429	0.87713	0.8729	(7Z,10Z,13Z,16Z,19Z)-docosapentaenoyl-CoA [m] + 10 CoA[m] + 5 FAD[m] + 10 H2O[m] + 10 NAD+[m] => 5 FADH2[m] + 10 H+[m] + 10 NADH[m] + 11 acetyl-CoA[m]	Beta oxidation of even-chain fatty acids (mitochondrial)
DW: HMR_3430	HMR_3430	0.85699	0.85276	(4Z,7Z,10Z,13Z,16Z,19Z)-docosahexaenoyl-CoA[m] + 10 CoA[m] + 4 FAD[m] + 10 H2O[m] + 10 NAD+[m] => 4 FADH2[m] + 10 H+[m] + 10 NADH[m] + 11 acetyl-CoA[m]	Beta oxidation of even-chain fatty acids (mitochondrial)
DW: HMR_3426	HMR_3426	0.63561	0.63529	8 CoA[m] + 5 FAD[m] + 8 H2O[m] + 8 NAD+[m] + linolenoyl-CoA[m] => 5 FADH2[m] + 8 H+[m] + 8 NADH[m] + 9 acetyl-CoA[m]	Beta oxidation of even-chain fatty acids (mitochondrial)
DW: HMR_3151	HMR_3151	0.49197	0.48607	(S)-hydroxyoctanoyl-CoA[m] + NAD+[m] => 3-oxooctanoyl-CoA[m] + H+[m] + NADH[m]	Beta oxidation of even-chain fatty acids (mitochondrial)
DW: HMR_3158	HMR_3158	0.49197	0.48607	(S)-hydroxyhexanoyl-CoA[m] + NAD+[m] => 3-oxohexanoyl-CoA[m] + H+[m] + NADH[m]	Beta oxidation of even-chain fatty acids (mitochondrial)
DW: HMR_3150	HMR_3150	0.49194	0.48607	(2E)-octenoyl-CoA[m] + H2O[m] => (S)-hydroxyoctanoyl-CoA[m]	Beta oxidation of even-chain fatty acids (mitochondrial)
DW: HMR_3157	HMR_3157	0.49194	0.48607	(2E)-hexenoyl-CoA[m] + H2O[m] => (S)-hydroxyhexanoyl-CoA[m]	Beta oxidation of even-chain fatty acids (mitochondrial)
DW: HMR_3149	HMR_3149	0.49163	0.48607	FAD[m] + octanoyl-CoA[m] => (2E)-octenoyl-CoA[m] + FADH2[m]	Beta oxidation of even-chain fatty acids (mitochondrial)
DW: HMR_3153	HMR_3153	0.49152	0.48607	3-oxooctanoyl-CoA[m] + CoA[m] => acetyl-CoA[m] + hexanoyl-CoA[m]	Beta oxidation of even-chain fatty acids (mitochondrial)
DW: HMR_3156	HMR_3156	0.46948	0.48607	FAD[m] + hexanoyl-CoA[m] => (2E)-hexenoyl-CoA[m] +	Beta oxidation of even-chain fatty

				FADH2[m]	acids (mitochondrial)
DW: HMR_3144	HMR_3144	0.46685	0.46618	(S)-hydroxydecanoyl-CoA[m] + NAD+[m] => 3-oxodecanoyl-CoA[m] + H+[m] + NADH[m]	Beta oxidation of even-chain fatty acids (mitochondrial)
DW: HMR_3143	HMR_3143	0.46682	0.46618	(2E)-decenoyl-CoA[m] + H2O[m] => (S)-hydroxydecanoyl-CoA[m]	Beta oxidation of even-chain fatty acids (mitochondrial)
DW: HMR_3146	HMR_3146	0.46642	0.46618	3-oxodecanoyl-CoA[m] + CoA[m] => acetyl-CoA[m] + octanoyl-CoA[m]	Beta oxidation of even-chain fatty acids (mitochondrial)
DW: HMR_3137	HMR_3137	0.43832	0.43856	(S)-3-hydroxydodecanoyl-CoA[m] + NAD+[m] => 3-oxododecanoyl-CoA[m] + H+[m] + NADH[m]	Beta oxidation of even-chain fatty acids (mitochondrial)
DW: HMR_3142	HMR_3142	0.4383	0.43856	FAD[m] + decanoyl-CoA[m] => (2E)-decenoyl-CoA[m] + FADH2[m]	Beta oxidation of even-chain fatty acids (mitochondrial)
DW: HMR_3139	HMR_3139	0.43792	0.43856	3-oxododecanoyl-CoA[m] + CoA[m] => acetyl-CoA[m] + decanoyl-CoA[m]	Beta oxidation of even-chain fatty acids (mitochondrial)
DW: HMR_3136	HMR_3136	0.436	0.43856	(2E)-dodecenoyl-CoA[m] + H2O[m] => (S)-3-hydroxydodecanoyl-CoA[m]	Beta oxidation of even-chain fatty acids (mitochondrial)
DW: HMR_3123	HMR_3123	0.4174	0.43302	(S)-3-hydroxyhexadecanoyl-CoA[m] + NAD+[m] => 3-oxopalmitoyl-CoA[m] + H+[m] + NADH[m]	Beta oxidation of even-chain fatty acids (mitochondrial)
DW: HMR_3125	HMR_3125	0.41702	0.43302	3-oxopalmitoyl-CoA[m] + CoA[m] => acetyl-CoA[m] + myristoyl-CoA[m]	Beta oxidation of even-chain fatty acids (mitochondrial)
DW: HMR_3122	HMR_3122	0.41519	0.43302	(2E)-hexadecenoyl-CoA[m] + H2O[m] => (S)-3-hydroxyhexadecanoyl-CoA[m]	Beta oxidation of even-chain fatty acids (mitochondrial)
DW: HMR_3121	HMR_3121	0.41389	0.43285	FAD[m] + palmitoyl-CoA[m] => (2E)-hexadecenoyl-CoA[m] + FADH2[m]	Beta oxidation of even-chain fatty acids (mitochondrial)
DW: HMR_3130	HMR_3130	0.35685	0.36018	(S)-3-hydroxytetradecanoyl-CoA[m] + NAD+[m] => 3-oxotetradecanoyl-CoA[m] + H+[m] + NADH[m]	Beta oxidation of even-chain fatty acids (mitochondrial)
DW: HMR_3132	HMR_3132	0.35653	-	3-oxotetradecanoyl-CoA[m] + CoA[m] => acetyl-CoA[m] + lauroyl-CoA[m]	Beta oxidation of even-chain fatty acids (mitochondrial)
DW: HMR_3128	HMR_3128	0.35618	-	FAD[m] + myristoyl-CoA[m] => (2E)-tetradecenoyl-CoA[m] + FADH2[m]	Beta oxidation of even-chain fatty acids (mitochondrial)
DW: HMR_3129	HMR_3129	0.35497	0.36018	(2E)-tetradecenoyl-CoA[m] + H2O[m] => (S)-3-hydroxytetradecanoyl-CoA[m]	Beta oxidation of even-chain fatty acids (mitochondrial)
DW: HMR_3421	HMR_3421	0.28607	-	(7Z,10Z,13Z,16Z)-docosatetraenoyl-CoA[m] + 10 CoA[m] + 6 FAD[m] + 10 H2O[m] + 10 NAD+[m] => 6 FADH2[m] + 10 H+[m] + 10 NADH[m] + 11 acetyl-CoA[m]	Beta oxidation of even-chain fatty acids (mitochondrial)
DW: HMR_3228	HMR_3228	0.7113	0.65169	(S)-3-hydroxyoleyleoyl-CoA[m] + NAD+[m] => 3-oxooleoyl-CoA[m] + H+[m] + NADH[m]	Beta oxidation of unsaturated fatty acids (n-9) (mitochondrial)

DW: HMR_3229	HMR_3229	0.71066	0.65169	3-oxooleoyl-CoA[m] + CoA[m] => 7-hexadecenoyl-CoA[m] + acetyl-CoA[m]	Beta oxidation of unsaturated fatty acids (n-9) (mitochondrial)
DW: HMR_3227	HMR_3227	0.70755	0.65169	H2O[m] + trans,cis-octadeca-2,9-dienoyl-CoA[m] => (S)-3-hydroxyoleyleoyl-CoA[m]	Beta oxidation of unsaturated fatty acids (n-9) (mitochondrial)
DW: HMR_3226	HMR_3226	0.70534	0.65143	FAD[m] + oleoyl-CoA[m] => FADH2[m] + trans,cis-octadeca-2,9-dienoyl-CoA[m]	Beta oxidation of unsaturated fatty acids (n-9) (mitochondrial)
DW: HMR_3232	HMR_3232	0.46866	0.47298	(S)-3-hydroxy-7-hexadecenoyl-CoA[m] + NAD+[m] => 3-oxo-7-hexadecenoyl-CoA[m] + H+[m] + NADH[m]	Beta oxidation of unsaturated fatty acids (n-9) (mitochondrial)
DW: HMR_3233	HMR_3233	0.46824	0.47298	3-oxo-7-hexadecenoyl-CoA[m] + CoA[m] => 5-tetradecenoyl-CoA[m] + acetyl-CoA[m]	Beta oxidation of unsaturated fatty acids (n-9) (mitochondrial)
DW: HMR_3230	HMR_3230	0.46778	0.47298	7-hexadecenoyl-CoA[m] + FAD[m] => FADH2[m] + trans,cis-hexadeca-2,7-dienoyl-CoA[m]	Beta oxidation of unsaturated fatty acids (n-9) (mitochondrial)
DW: HMR_3231	HMR_3231	0.46619	0.47298	H2O[m] + trans,cis-hexadeca-2,7-dienoyl-CoA[m] => (S)-3-hydroxy-7-hexadecenoyl-CoA[m]	Beta oxidation of unsaturated fatty acids (n-9) (mitochondrial)
DW: HMR_3239	HMR_3239	0.38349	0.38711	(2E)-dodecenoyl-CoA[m] <=> (3Z)-dodecenoyl-CoA[m]	Beta oxidation of unsaturated fatty acids (n-9) (mitochondrial)
DW: HMR_3236	HMR_3236	0.38349	0.38711	NAD+[m] + cis-(3S)-hydroxytetradec-5-enoyl-CoA[m] => 3-oxomyrist-5-enoyl-CoA[m] + H+[m] + NADH[m]	Beta oxidation of unsaturated fatty acids (n-9) (mitochondrial)
DW: HMR_3237	HMR_3237	0.38314	0.38711	3-oxomyrist-5-enoyl-CoA[m] + CoA[m] => (3Z)-dodecenoyl-CoA[m] + acetyl-CoA[m]	Beta oxidation of unsaturated fatty acids (n-9) (mitochondrial)
DW: HMR_3234	HMR_3234	0.38277	0.38711	5-tetradecenoyl-CoA[m] + FAD[m] => FADH2[m] + trans,cis-myristo-2,5-dienoyl-CoA[m]	Beta oxidation of unsaturated fatty acids (n-9) (mitochondrial)
DW: HMR_3235	HMR_3235	0.38146	0.38711	H2O[m] + trans,cis-myristo-2,5-dienoyl-CoA[m] => cis-(3S)-hydroxytetradec-5-enoyl-CoA[m]	Beta oxidation of unsaturated fatty acids (n-9) (mitochondrial)
DW: HMR_4137	HMR_4137	0.74141	0.72378	CoA[m] + NAD+[m] + pyruvate[m] => CO2[m] + H+[m] + NADH[m] + acetyl-CoA[m]	Glycolysis / Gluconeogenesis
DW: HMR_3212	HMR_3212	0.63657	0.62132	FAD[m] + propanoyl-CoA[m] => FADH2[m] + acrylyl-CoA[m]	Propanoate metabolism
DW: HMR_4735	HMR_4735	0.63601	0.61992	H2O[m] + acrylyl-CoA[m] => 3-hydroxypropionyl-CoA[m]	beta-Alanine metabolism
DW: HMR_4741	HMR_4741	0.60374	0.61992	3-hydroxypropionyl-CoA[m] + H2O[m] => CoA[m] + hydracrylate[m]	Propanoate metabolism
DW: HMR_2726	HMR_2726	-	0.48967	(7Z,10Z,13Z,16Z,19Z)-docosapentaenoyl-CoA [c] + L-carnitine[c] <=> (7Z,10Z,13Z,16Z,19Z)-docosapentaenoylcarnitine[c] + CoA[c]	Carnitine shuttle (cytosolic)
DW: HMR_2730	HMR_2730	-	0.47837	(4Z,7Z,10Z,13Z,16Z,19Z)-docosahexaenoyl-CoA[c] + L-carnitine[c] <=> CoA[c] + docosahexaenoylcarnitine[c]	Carnitine shuttle (cytosolic)

DW: HMR_2742	HMR_2742	-	0.43985	CoA[c] + linoleic-carnitine[c] <=> L-carnitine[c] + linoleoyl-CoA[c]	Carnitine shuttle (cytosolic)
DW: HMR_2727	HMR_2727	-	0.68675	(7Z,10Z,13Z,16Z,19Z)-docosapentaenoylcarnitine[c] + L-carnitine[m] <=> (7Z,10Z,13Z,16Z,19Z)-docosapentaenoylcarnitine[m] + L-carnitine[c]	Carnitine shuttle (mitochondrial)
DW: HMR_2731	HMR_2731	-	0.67091	L-carnitine[c] + docosahexaenoylcarnitine[m] <=> L-carnitine[m] + docosahexaenoylcarnitine[c]	Carnitine shuttle (mitochondrial)
DW: HMR_2744	HMR_2744	-	0.61688	L-carnitine[c] + linoleic-carnitine[m] <=> L-carnitine[m] + linoleic-carnitine[c]	Carnitine shuttle (mitochondrial)
DW: HMR_2722	HMR_2722	-	0.53418	(5Z,8Z,11Z,14Z,17Z)-eicosapentaenoylcarnitine[c] + L-carnitine[m] <=> (5Z,8Z,11Z,14Z,17Z)-eicosapentaenoylcarnitine[m] + L-carnitine[c]	Carnitine shuttle (mitochondrial)
DW: HMR_2712	HMR_2712	-	0.49981	L-carnitine[c] + octadecatrienoylcarnitine[m] <=> L-carnitine[m] + octadecatrienoylcarnitine[c]	Carnitine shuttle (mitochondrial)
DW: HMR_2729	HMR_2729	-	0.43168	(7Z,10Z,13Z,16Z,19Z)-docosapentaenoyl-CoA [m] + L-carnitine[m] <=> (7Z,10Z,13Z,16Z,19Z)-docosapentaenoylcarnitine[m] + CoA[m]	Carnitine shuttle (mitochondrial)
DW: HMR_2732	HMR_2732	-	0.42172	(4Z,7Z,10Z,13Z,16Z,19Z)-docosahexaenoyl-CoA[m] + L-carnitine[m] <=> CoA[m] + docosahexaenoylcarnitine[m]	Carnitine shuttle (mitochondrial)
DW: HMR_2745	HMR_2745	-	0.38776	CoA[m] + linoleic-carnitine[m] <=> L-carnitine[m] + linoleoyl-CoA[m]	Carnitine shuttle (mitochondrial)
DW: HMR_4295	HMR_4295	0.28472	-	ATP[m] + H+[m] + HCO3-[m] + acetyl-CoA[m] => ADP[m] + Pi[m] + malonyl-CoA[m]	Fatty acid biosynthesis (even-chain)
DW: HMR_4655	HMR_4655	0.30113	-	H+[c] + NADPH[c] + folate[c] <=> NADP+[c] + dihydrofolate[c]	Folate metabolism
DW: HMR_0534	HMR_0534	0.31576	-	linoleoyl-CoA[c] + sn-glycerol-3-phosphate[c] => 1-acylglycerol-3P-lin[c] + CoA[c]	Glycerolipid metabolism
DW: HMR_0453	HMR_0453	0.2867	-	H+[c] + NADPH[c] + glyceraldehyde[c] <=> NADP+[c] + glycerol[c]	Glycerolipid metabolism
DW: HMR_6409	HMR_6409	0.99937	0.99999	H+[m] + NADH[m] + lipoamide[m] <=> NAD+[m] + dihydrolipoamide[m]	Glycine, serine and threonine metabolism
DW: HMR_1263	HMR_1263	0.353	-	10,11-dihydro-LTB4-CoA[c] + AMP[c] + PPi[c] <=> 10,11-dihydro-LTB4[c] + ATP[c] + CoA[c]	Leukotriene metabolism
DW: HMR_1264	HMR_1264	0.353	-	10,11-dihydro-LTB4-CoA[m] + AMP[m] + PPi[m] <=> 10,11-dihydro-LTB4[m] + ATP[m] + CoA[m]	Leukotriene metabolism
DW: HMR_6914	HMR_6914	0.99879	0.99874	8 H+[m] + O2[m] + 4 ferrocytochrome C[m] => 4 H+[c] + 2	Oxidative phosphorylation

				H2O[m] + 4 ferricytochrome C[m]	
DW: HMR_6918	HMR_6918	0.9985	0.99838	2 H+[m] + 2 ferricytochrome C[m] + ubiquinol[m] => 4 H+[c] + 2 ferrocytochrome C[m] + ubiquinone[m]	Oxidative phosphorylation
DW: HMR_6921	HMR_6921	0.81528	0.80292	5 H+[m] + NADH[m] + ubiquinone[m] => 4 H+[c] + NAD+[m] + ubiquinol[m]	Oxidative phosphorylation
DW: HMR_6912	HMR_6912	0.44949	0.45579	H2O[m] + PPi[m] => 2 Pi[m]	Oxidative phosphorylation
DW: HMR_4004	HMR_4004	0.44612	0.45408	2 ADP[m] <=> AMP[m] + ATP[m]	Purine metabolism
DW: HMR_4002	HMR_4002	0.35411	0.37963	2 ADP[c] <=> AMP[c] + ATP[c]	Purine metabolism
DW: HMR_0007	HMR_0007	0.79255	0.99996	H2O[s] + TAG-VLDL pool[s] => 1,2-diacylglycerol-VLDL pool[s] + fatty acid-VLDL pool[s]	Transport, extracellular
DW: HMR_0008	HMR_0008	0.79255	0.99996	1,2-diacylglycerol-VLDL pool[s] + H2O[s] => 1-acylglycerol-VLDL pool[s] + fatty acid-VLDL pool[s]	Transport, extracellular
DW: HMR_4885	HMR_4885	0.78151	0.95409	H2O[c] <=> H2O[s]	Transport, extracellular
DW: HMR_8741	HMR_8741	0.6218	0.64492	fumarate[c] + sulfite[m] <=> fumarate[m] + sulfite[c]	Transport, mitochondrial
DW: HMR_5043	HMR_5043	0.55156	0.55363	H+[c] + Pi[c] <=> H+[m] + Pi[m]	Transport, mitochondrial
DW: HMR_4888	HMR_4888	0.44237	-	H2O[c] <=> H2O[m]	Transport, mitochondrial
DW: HMR_6330	HMR_6330	0.34258	-	AKG[c] + Pi[m] <=> AKG[m] + Pi[c]	Transport, mitochondrial
DW: HMR_4145	HMR_4145	0.99859	0.99915	CoA[m] + citrate[m] <=> H2O[m] + OAA[m] + acetyl-CoA[m]	Tricarboxylic acid cycle and glyoxylate/dicarboxylate metabolism
DW: HMR_4209	HMR_4209	0.97892	0.99998	AKG[m] + thiamin-PP[m] => 3-carboxy-1-hydroxypropyl-ThPP[m] + CO2[m]	Tricarboxylic acid cycle and glyoxylate/dicarboxylate metabolism
DW: HMR_6413	HMR_6413	0.97892	0.99998	3-carboxy-1-hydroxypropyl-ThPP[m] + lipoamide[m] => S-succinyldihydrolipoamide[m] + thiamin-PP[m]	Tricarboxylic acid cycle and glyoxylate/dicarboxylate metabolism
DW: HMR_6414	HMR_6414	0.88607	0.66094	CoA[m] + S-succinyldihydrolipoamide[m] <=> dihydrolipoamide[m] + succinyl-CoA[m]	Tricarboxylic acid cycle and glyoxylate/dicarboxylate metabolism
DW: HMR_4456	HMR_4456	0.85545	0.99999	citrate[m] <=> isocitrate[m]	Tricarboxylic acid cycle and glyoxylate/dicarboxylate metabolism
DW: HMR_4408	HMR_4408	0.82782	0.82864	H2O[c] + fumarate[c] <=> malate[c]	Tricarboxylic acid cycle and glyoxylate/dicarboxylate

					metabolism
DW: HMR_3958	HMR_3958	0.82237	0.92893	NADP+[m] + isocitrate[m] => AKG[m] + CO2[m] + H+[m] + NADPH[m]	Tricarboxylic acid cycle and glyoxylate/dicarboxylate metabolism
DW: HMR_4652	HMR_4652	0.72097	0.71081	fumarate[m] + ubiquinol[m] <=> succinate[m] + ubiquinone[m]	Tricarboxylic acid cycle and glyoxylate/dicarboxylate metabolism
DW: HMR_8743	HMR_8743	0.4344	0.43467	FADH2[m] + fumarate[m] <=> FAD[m] + succinate[m]	Tricarboxylic acid cycle and glyoxylate/dicarboxylate metabolism
DW: HMR_4147	HMR_4147	0.37268	-	CoA[m] + GTP[m] + succinate[m] <=> GDP[m] + Pi[m] + succinyl-CoA[m]	Tricarboxylic acid cycle and glyoxylate/dicarboxylate metabolism
DW: HMR_3160	HMR_3160	0.49152	0.48607	3-oxohexanoyl-CoA[m] + CoA[m] => acetyl-CoA[m] + butyryl-CoA[m]	Beta oxidation of even-chain fatty acids (mitochondrial)
DW: HMR_3163	HMR_3163	0.49197	0.48607	FAD[m] + butyryl-CoA[m] => FADH2[m] + crotonyl-CoA[m]	Butanoate metabolism
DW: HMR_3164	HMR_3164	0.49194	0.48607	H2O[m] + crotonyl-CoA[m] => (S)-3-hydroxybutyryl-CoA[m]	Tryptophan metabolism
DW: HMR_3166	HMR_3166	0.49197	0.48607	(S)-3-hydroxybutyryl-CoA[m] + NAD+[m] => H+[m] + NADH[m] + acetoacetyl-CoA[m]	Tryptophan metabolism
DW: HMR_3215	HMR_3215	0.42563	0.43453	(R)-methylmalonyl-CoA[m] => succinyl-CoA[m]	Valine, leucine, and isoleucine metabolism
DW: HMR_3213	HMR_3213	-	0.4213	methylmalonyl-CoA[m] => (R)-methylmalonyl-CoA[m]	Valine, leucine, and isoleucine metabolism

Supplementary Figures

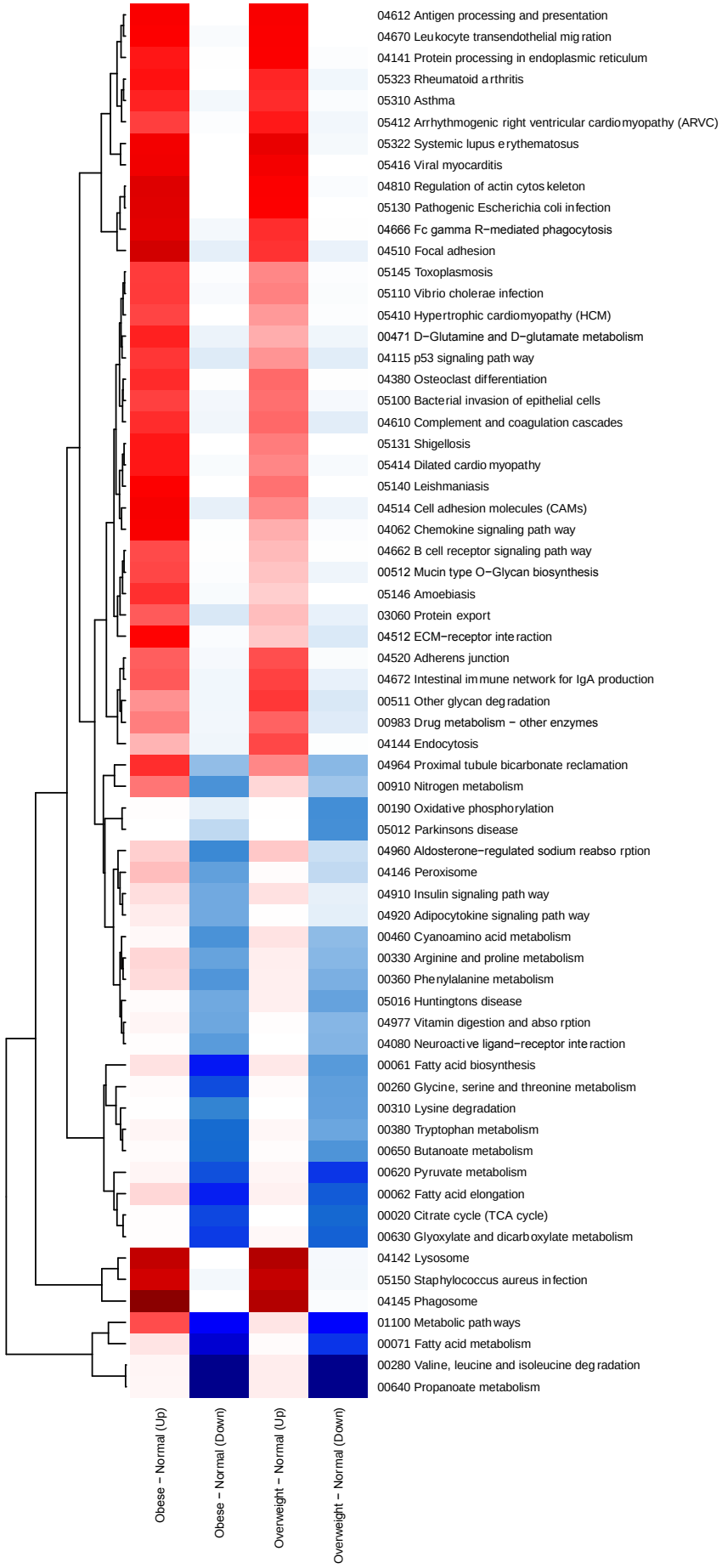

Figure S1. Enrichment in KEGG pathways between obese, overweight and normal (lean) male subjects, as calculated by the Reporter Features algorithm. Red and blue represent enrichment in up-regulated and down-regulated genes respectively. Deep red/blue represents 1e-20.

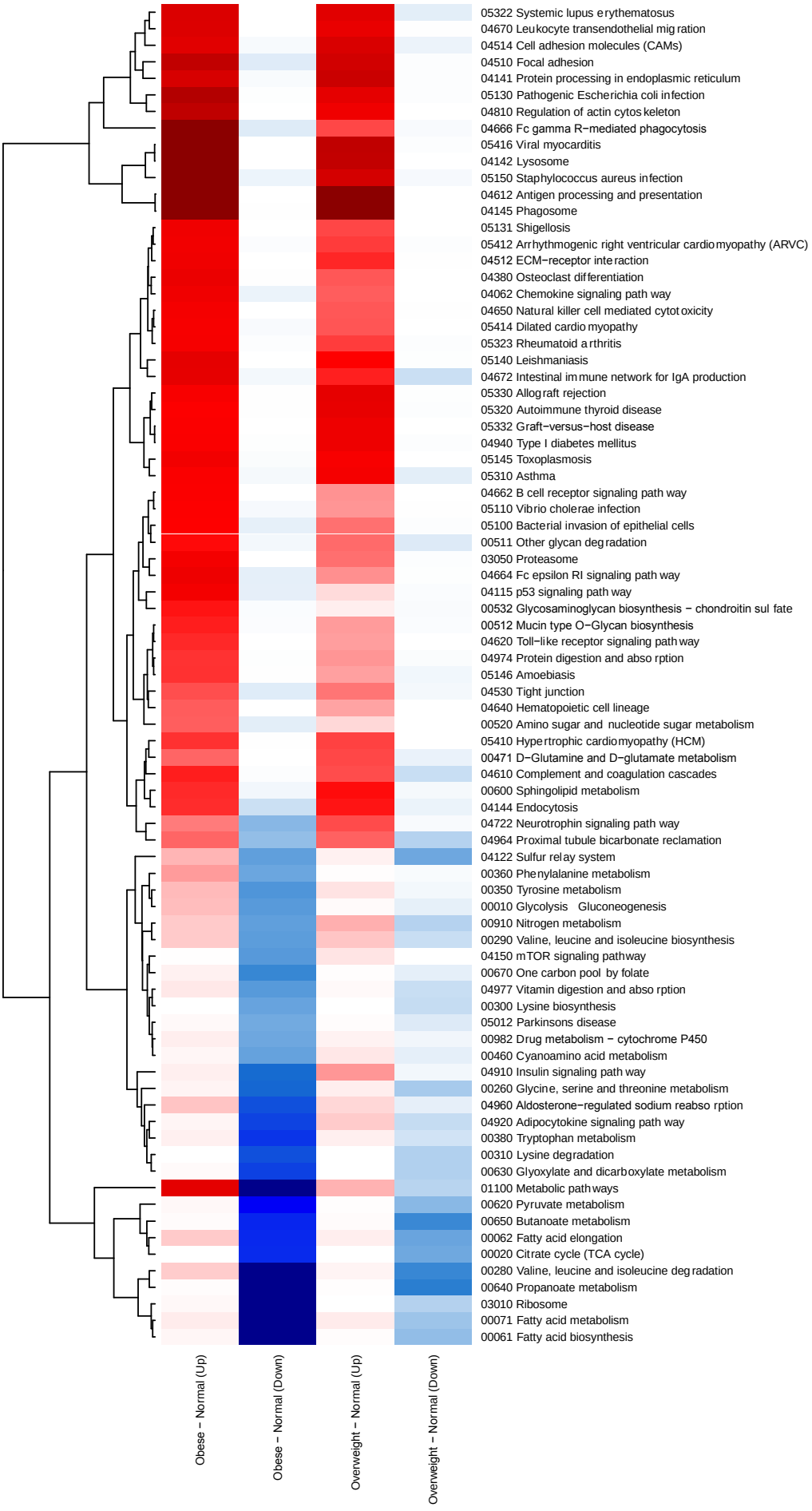

Figure S2. Enrichment in KEGG pathways between obese, overweight and normal (lean) female subjects, as calculated by the Reporter Features algorithm. Red and blue represent enrichment in up-regulated and down-regulated genes respectively. Deep red/blue represents 1e-20.

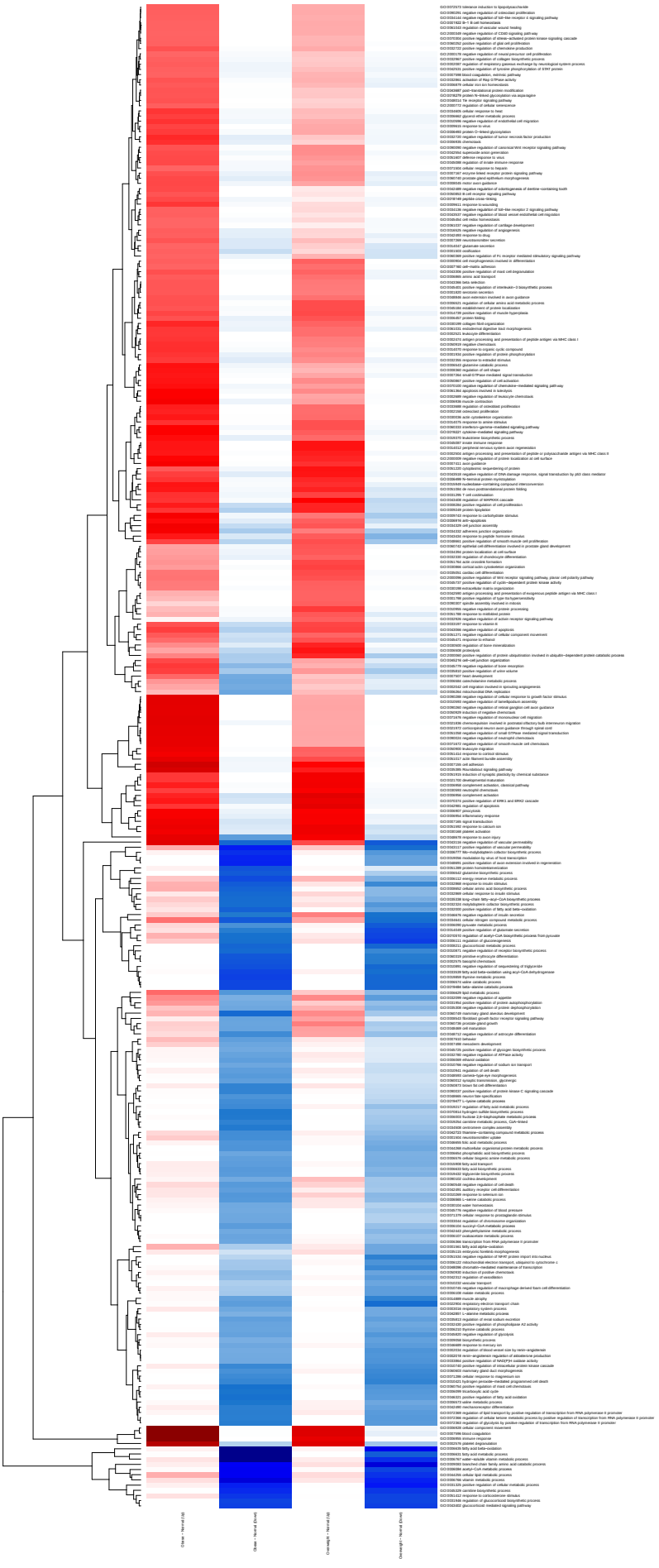

Figure S3. Enrichment in biological process Gene Ontology (BP:GO) terms between obese, overweight and normal (lean) male subjects, as calculated by the Reporter Features algorithm. Red and blue represent enrichment in up-regulated and down-regulated genes respectively. Deep red/blue represents 1e-20.

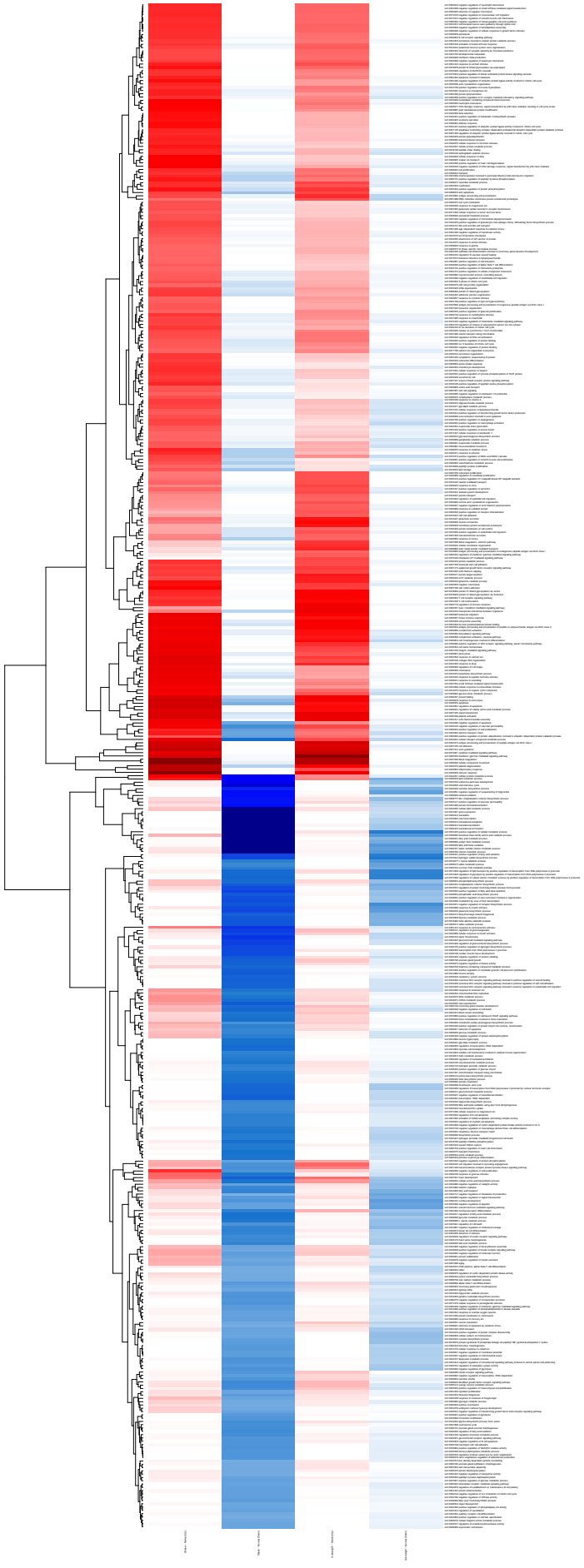

Figure S4. Enrichment in biological process Gene Ontology (BP:GO) terms between obese, overweight and normal (lean) female subjects, as calculated by the Reporter Features algorithm. Red and blue represent enrichment in up-regulated and down-regulated genes respectively. Deep red/blue represents 1e-20.

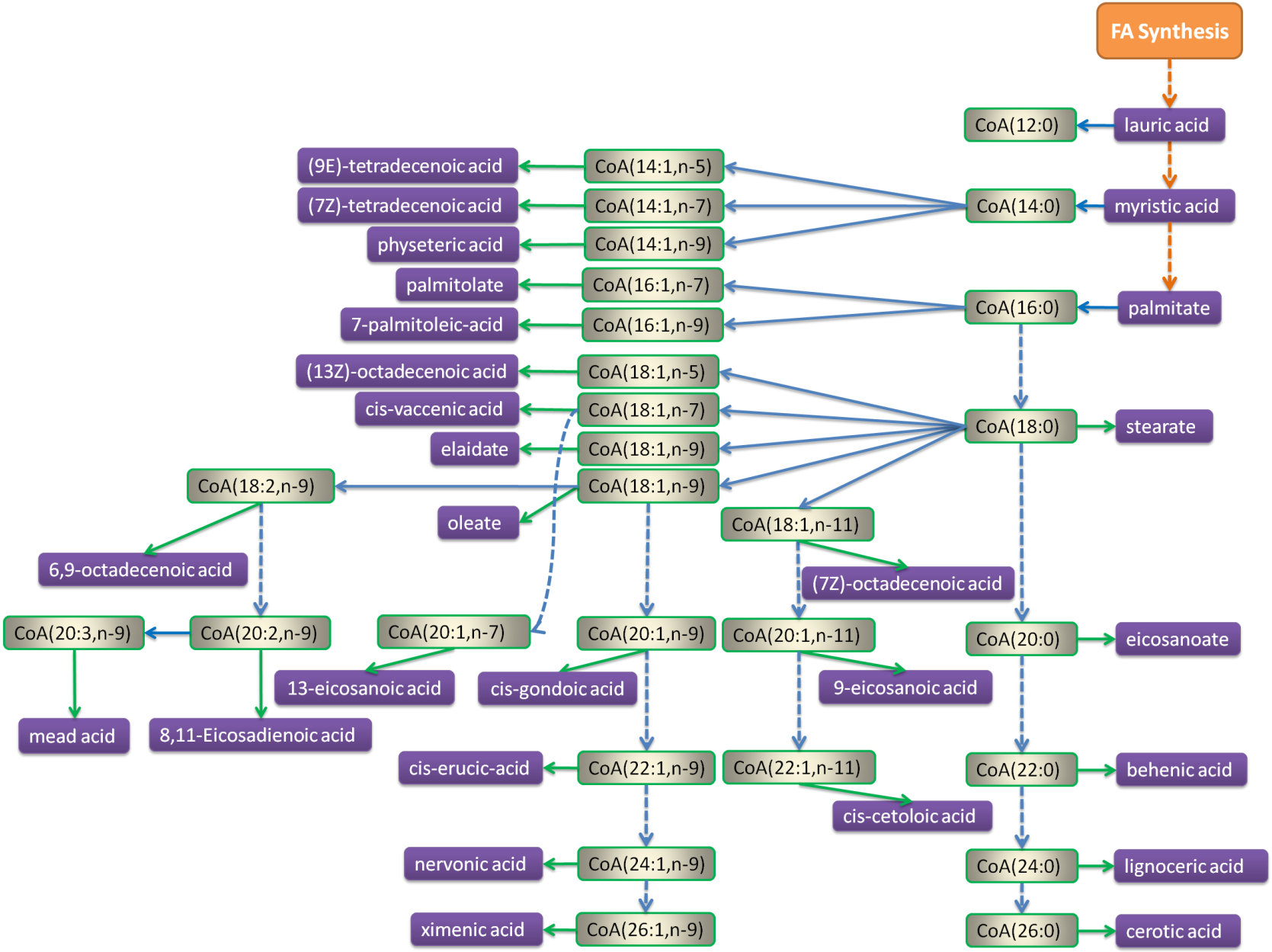

Figure S5. Illustration of omega 9 and other fatty acids metabolism in the genome-scale metabolic model for adipocytes, *iAdipocytes1809*.

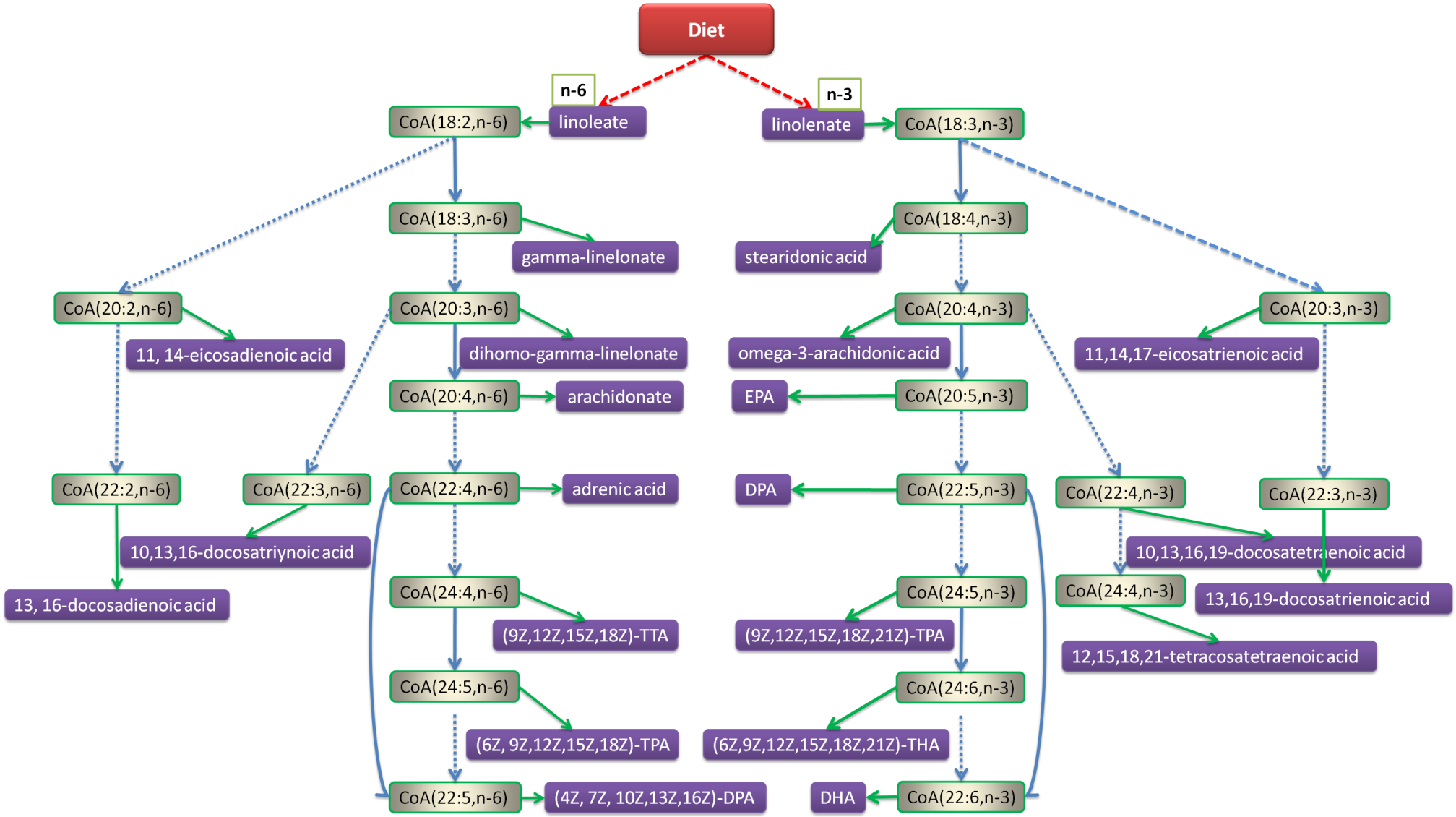

Figure S6. Illustration of linoleate (LA), unsaturated omega-6 fatty acid and linolenate (ALA), polyunsaturated omega-3 fatty acid acids metabolism in the genome-scale metabolic model for adipocytes, *iAdipocytes1809.* LA and ALA are essential fatty acids and should be taken with the diet.

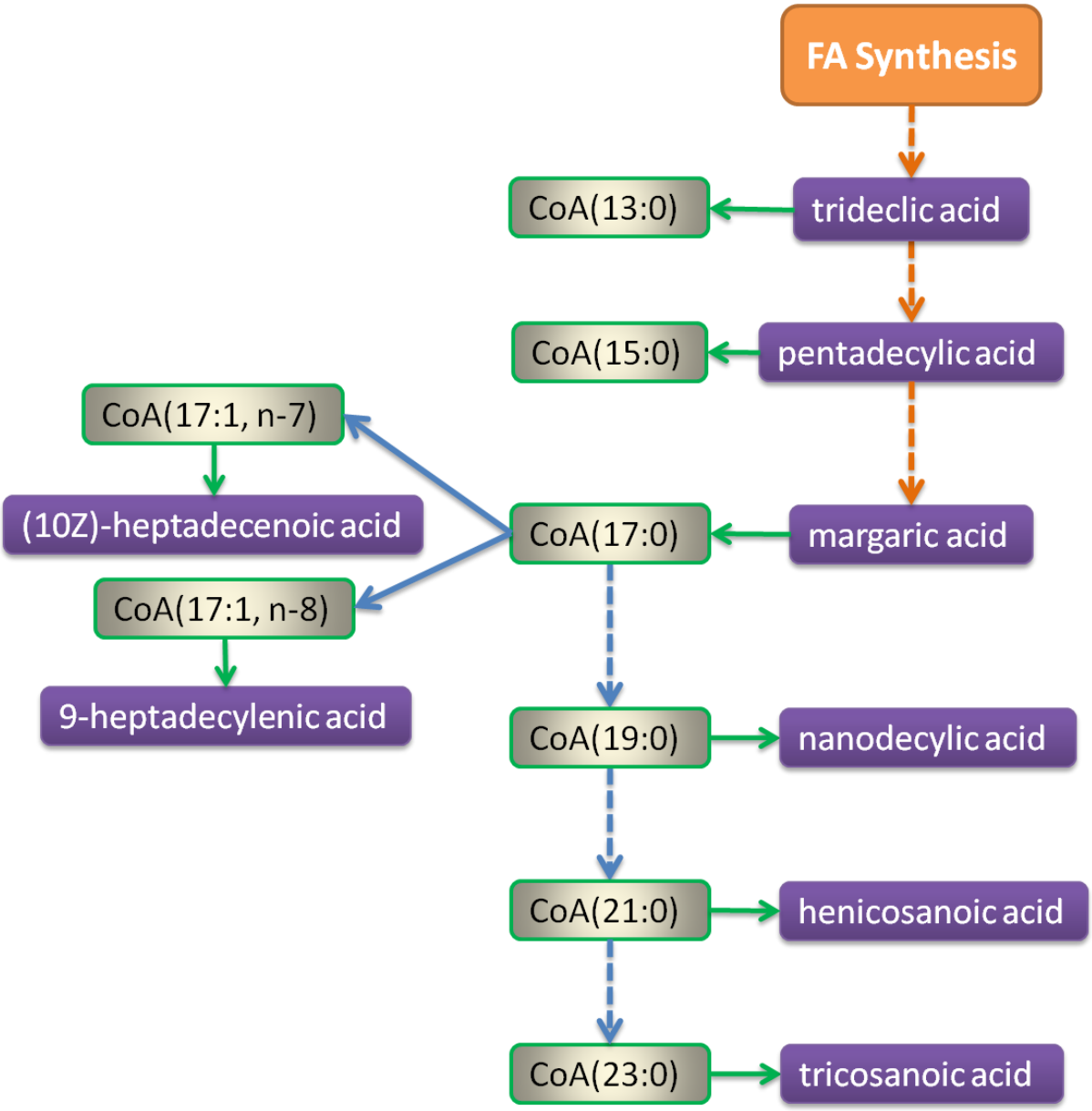

Figure S7. Illustration of odd chain fatty acids metabolism in the genome-scale metabolic model for adipocytes, *iAdipocytes1809.*

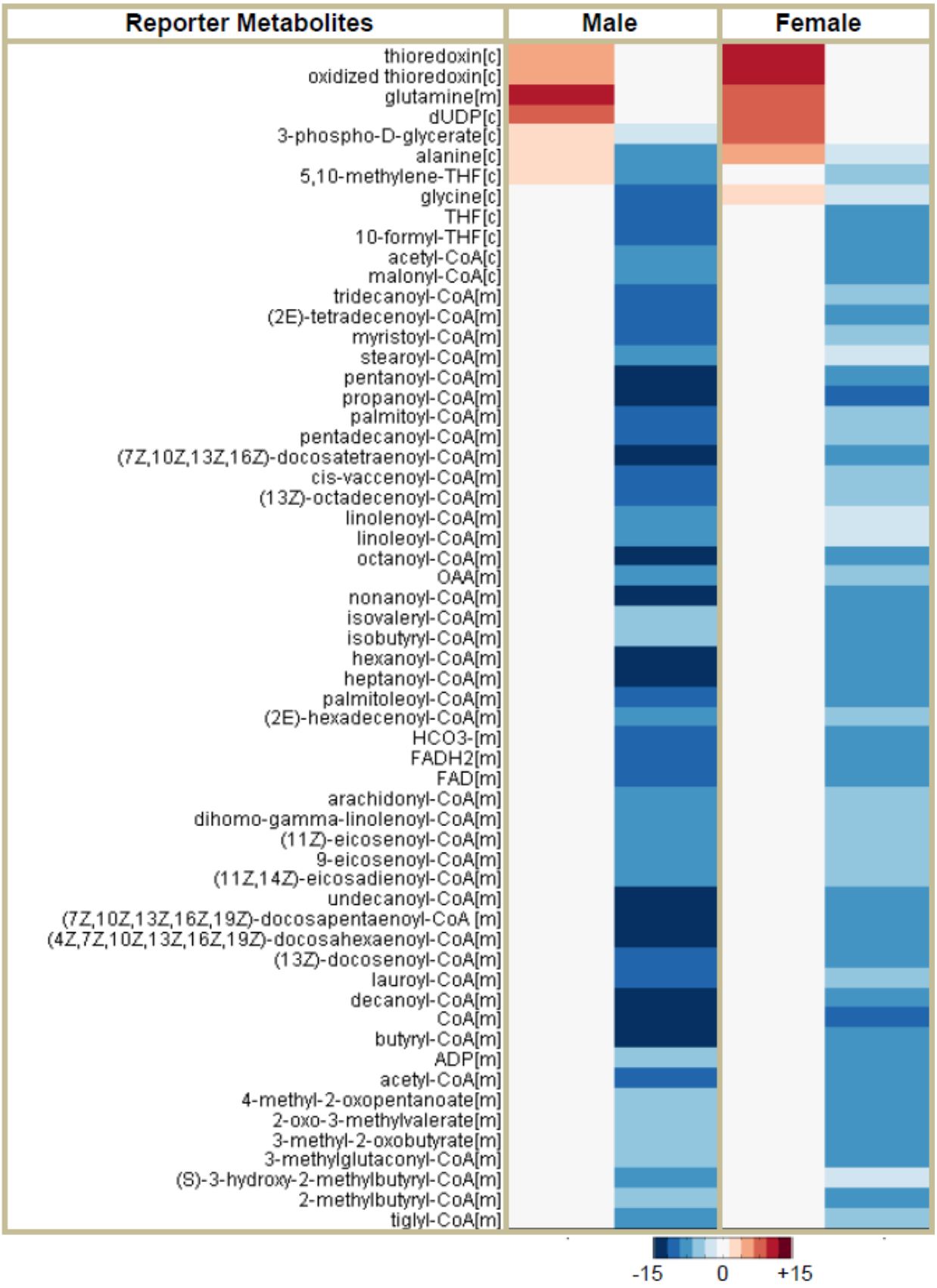

Figure S8. Reporter Metabolites obtained in the same way as in Figure 5, but using the previously published GEM, *iAB586*. Metabolites with p-values lower than 6e-3 are shown, rather than the top 20 metabolites, since there were only a few metabolites around which the genes were significantly up regulated.

Supplementary Datasets

Dataset 1a. The presence/absence of proteins encoded by 14,077 genes in adipocytes is examined based on immunohistochemistry and using antibodies generated within the Human Protein Atlas (HPA) project.

Dataset 1b. Xie et. al. (Xie et al., 2010) characterized the proteome of human adipocytes and reported existence of proteins encoded by 1,574 genes in subcutaneous abdominal adipocytes taken from three healthy lean subjects.

Dataset 1c. The enzymes reported in the Human Protein Atlas database (http://www.proteinatlas.org) are listed.

Dataset 2a. Subcellular localization of the proteins based on the Human Protein Atlas (HPA) and Uniprot data and their assignments in the genome-scale metabolic model for adipocytes, *iAdipocytes1809.*

Dataset 2b. Subcellular localization of the proteins and their confidence scores in the genome-scale metabolic model for adipocytes, *iAdipocytes1809* based on the Human Protein Atlas (HPA) and Uniprot data. Confidence score 2 for HPA, 1 for Uniprot and 3 for both HPA and Uniprot were assigned for each protein.

Dataset 3. Enrichment of biological process Gene Ontology terms for encoded genes in here generated and previously published proteome data (assessed with DAVID (Huang et al., 2009)) are compared with the biological process Gene Ontology terms enrichment results of encoded genes in transcriptome data in male and female subjects.

Dataset 4. List of the input metabolites and inferred transport reactions in the genome-scale metabolic model for adipocytes, *iAdipocytes1809,* to ensure the connectivity.

Dataset 5. Known biological function of the adipocytes and the metabolic capacity was demonstrated by the simulation of 250 metabolic functions based on the definition of functions in HepatoNet 1 (Gille et al., 2010).

Dataset 6. McQuaid et al. (McQuaid et al., 2011) measured the delivery and transport of fatty acids in adipose tissue using multiple and simultaneous stable-isotope fatty acid tracers in lean and obese subjects groups over a 24 hour period. Even though abdominally obese subjects have greater adipose tissue mass than lean control subjects, the rates of delivery of NEFAs are down regulated in obese subjects. In their study, uptake/secretion rates for NEFAs, TAGs and glucose in obese and lean subjects are reported. In adipose tissue, blood flow, glucose uptake, release of NEFAs and the extraction of TAGs from plasma was significantly lower in the abdominally obese subjects compared to lean subjects. Values are given as means ± SD.

Dataset 7. Paterson et. al (Patterson et al., 2002) have studied the forearm and adipose tissue amino acid metabolism in lean and obese human subjects after 22 hours of fasting. They hypothesized that greater conservation of body protein observed during fasting in obese than in lean subjects and a combination of stable isotope tracer infusion and arteriovenous balance

techniques was used to quantify amino acid kinetics. In their study, local net amino acid arteriovenous differences were calculated as the amino acid concentration in arterial plasma minus the concentration in venous plasma and local net fluxes were calculated as the arteriovenous difference multiplied by local plasma flow. Plasma arterial amino acid concentrations, regional subcutaneous abdominal adipose tissue arteriovenous concentration differences are adapted from the study of Paterson et. al (Patterson et al., 2002) and local net fluxes for lean and obese subjects were calculated.

Dataset 8. Fatty acid (FA) composition in human plasma (Quehenberger et al., 2010), adipose tissue (Hodson et al., 2008; Raclot et al., 1997) and liver tissue (Shorten and Upreti, 2005) where there is not any information for adipocytes are incorporated in to the model for generation of pool reactions. Lipidomics analysis of a pooled human plasma obtained from healthy individuals after overnight fasting has been used in the model (Quehenberger et al., 2010). In their study, over 500 distinct molecular species distributed among the main lipid categories including fatty acyls, glycerolipids, glycerophospholipids, sphingolipids, sterols, and prenols were quantified. The reported 31 FAs in human plasma used in our model and normalized values are shown. In their study, some plasma FA known to exist in the structure of adipose tissue triacylglycerols and phospholipids have not been reported. These unreported FAs were included in to the structure of pool reactions by assuming their concentrations as half of the minimum concentration reported in the measurement study. Assumptions for the concentration of non reported FAs in lipidomics analysis allow us to include them into the genome-scale metabolic model for adipocytes, *iAdipocytes1809*. Raclot et. al. (Raclot et al., 1997) measured the FA composition of TAG in adipose tissue and originated non-esterified FA (NEFA) concentration from adipose TAGs through lipolysis. The mobilization of 34 individual fatty acids is quantified in adipose tissue of eight healthy non-obese women and used in our model to generate the pool reactions. The reported FA content was normalized to 1 mol/mol of TAG and shown. Hodson et. al. (Hodson et al., 2008) collected the data for measurements of FA composition in adipose tissue and blood lipids and their changes with different diet. The reported FA composition of NEFA is compared with the lipidomics analysis of a pooled human plasma study (Quehenberger et al., 2010) and an agreement has been seen. The FA molar composition of plasma TAGs and CEs reported in the study is normalized to 1 and used in *iAdipocytes1809*.

Dataset 9a. Lipid droplet formation in adipose tissue of lean and obese subjects have been predicted with the genome-scale metabolic model for adipocytes, *iAdipocytes1809* and exchange reactions have been presented. Uptake/secretion rates for NEFA, TAG and glucose in obese and lean subjects are adapted from McQuaid et al. (McQuaid et al., 2011).

Dataset 9b. Acetyl-CoA formation in the mitochondria of adipose tissue in lean and obese subjects have been predicted through the usage of our genome-scale metabolic model for adipocytes, *iAdipocytes1809* and exchange reactions have been presented. Uptake/secretion rates for NEFA, TAG and glucose in obese and lean subjects are adapted from McQuaid et al. (McQuaid et al., 2011).

Supplementary References

Bartz, R., Li, W.H., Venables, B., Zehmer, J.K., Roth, M.R., Welti, R., Anderson, R.G.W., Liu, P.S., and Chapman, K.D. (2007). Lipidomics reveals that adiposomes store ether lipids and mediate phospholipid traffic. J Lipid Res *48*, 837-847.

Berardini, T.Z., Li, D.H., Huala, E., Bridges, S., Burgess, S., McCarthy, F., Carbon, S., Lewis, S.E., Mungall, C.J., Abdulla, A., *et al.* (2010). The Gene Ontology in 2010: extensions and refinements The Gene Ontology Consortium. Nucleic Acids Res *38*, D331-D335.

Bickerton, A.S.T., Roberts, R., Fielding, B.A., Hodson, L., Blaak, E.E., Wagenmakers, A.J.M., Gilbert, M., Karpe, F., and Frayn, K.N. (2007). Preferential uptake of dietary fatty acids in adipose tissue and muscle in the postprandial period. Diabetes *56*, 168-176.

Caballero, B. (2009). Guide to nutritional supplements (Oxford, UK, Elsevier/Academic Press).

Duncan, R.E., Ahmadian, M., Jaworski, K., Sarkadi-Nagy, E., and Sul, H.S. (2007). Regulation of lipolysis in adipocytes. Annu Rev Nutr *27*, 79-101.

Gille, C., Bolling, C., Hoppe, A., Bulik, S., Hoffmann, S., Hubner, K., Karlstadt, A., Ganeshan, R., Konig, M., Rother, K., *et al.* (2010). HepatoNet1: a comprehensive metabolic reconstruction of the human hepatocyte for the analysis of liver physiology. Mol Syst Biol *6*, 411.

Guilherme, A., Virbasius, J.V., Puri, V., and Czech, M.P. (2008). Adipocyte dysfunctions linking obesity to insulin resistance and type 2 diabetes. Nat Rev Mol Cell Bio *9*, 367-377.

Hodson, L., Skeaff, C.M., and Fielding, B.A. (2008). Fatty acid composition of adipose tissue and blood in humans and its use as a biomarker of dietary intake. Prog Lipid Res *47*, 348-380.

Huang, D.W., Sherman, B.T., and Lempicki, R.A. (2009). Systematic and integrative analysis of large gene lists using DAVID bioinformatics resources. Nat Protoc *4*, 44-57.

Kanehisa, M., Goto, S., Sato, Y., Furumichi, M., and Tanabe, M. (2012). KEGG for integration and interpretation of large-scale molecular data sets. Nucleic Acids Res *40*, D109-D114.

Large, V., Peroni, O., Letexier, D., Ray, H., and Beylot, M. (2004). Metabolism of lipids in human white adipocyte. Diabetes Metab *30*, 294-309.

McQuaid, S.E., Hodson, L., Neville, M.J., Dennis, A.L., Cheeseman, J., Humphreys, S.M., Ruge, T., Gilbert, M., Fielding, B.A., Frayn, K.N., *et al.* (2011). Downregulation of Adipose Tissue Fatty Acid Trafficking in Obesity A Driver for Ectopic Fat Deposition? Diabetes *60*, 47-55.

Mills, G.L., Lane, P.A., and Weech, P.K. (1984). A guidebook to lipoprotein technique (Amsterdam; New York, Sole distributors for the USA and Canada, Elsevier Science Pub. Co.).

Mitrou, P., Boutati, E., Lambadiari, V., Maratou, E., Papakonstantinou, A., Komesidou, V., Sidossis, L., Tountas, N., Katsilambros, N., Economopoulos, T., *et al.* (2009). Rates of Glucose Uptake in Adipose Tissue and Muscle in Vivo after a Mixed Meal in Women with Morbid Obesity. J Clin Endocr Metab *94*, 2958-2961.

Oliveira, A.P., Patil, K.R., and Nielsen, J. (2008). Architecture of transcriptional regulatory circuits is knitted over the topology of bio-molecular interaction networks. Bmc Syst Biol *2*.

Patil, K.R., and Nielsen, J. (2005). Uncovering transcriptional regulation of metabolism by using metabolic network topology. P Natl Acad Sci USA *102*, 2685-2689.

Patterson, B.W., Horowitz, J.F., Wu, G.Y., Watford, M., Coppack, S.W., and Klein, S. (2002). Regional muscle and adipose tissue amino acid metabolism in lean and obese women. Am J Physiol-Endoc M *282*, E931-E936.

Quehenberger, O., Armando, A.M., Brown, A.H., Milne, S.B., Myers, D.S., Merrill, A.H., Bandyopadhyay, S., Jones, K.N., Kelly, S., Shaner, R.L., *et al.* (2010). Lipidomics reveals a remarkable diversity of lipids in human plasma. J Lipid Res *51*, 3299-3305.
Raclot, T., Langin, D., Lafontan, M., and Groscolas, R. (1997). Selective release of human adipocyte fatty acids according to molecular structure. Biochem J *324 (Pt 3)*, 911-915.
Shorten, P.R., and Upreti, G.C. (2005). A mathematical model of fatty acid metabolism and VLDL assembly in human liver. Bba-Mol Cell Biol L *1736*, 94-108.
Strawford, A., Antelo, F., Christiansen, M., and Hellerstein, M.K. (2004). Adipose tissue triglyceride turnover, de novo lipogenesis, and cell proliferation in humans measured with (H2O)-H-2. Am J Physiol-Endoc M *286*, E577-E588.
Walley, A.J., Jacobson, P., Falchi, M., Bottolo, L., Andersson, J.C., Petretto, E., Bonnefond, A., Vaillant, E., Lecoeur, C., Vatin, V., *et al.* (2012). Differential coexpression analysis of obesity-associated networks in human subcutaneous adipose tissue. Int J Obesity *36*, 137-147.
Wellen, K.E., and Hotamisligil, G.S. (2003). Obesity-induced inflammatory changes in adipose tissue. J Clin Invest *112*, 1785-1788.
Xie, X.T., Yi, Z.P., Bowen, B., Wolf, C., Flynn, C.R., Sinha, S., Mandarino, L.J., and Meyer, C. (2010). Characterization of the Human Adipocyte Proteome and Reproducibility of Protein Abundance by One-Dimensional Gel Electrophoresis and HPLC-ESI-MS/MS. J Proteome Res *9*, 4521-4534.